IEEE Access
Multidisciplinary | Rapid Review | Open Access Journal

Received November 22, 2019, accepted December 28, 2019, date of publication December 31, 2019,
date of current version January 9, 2020.

Digital Object Identifier 10.1109/ACCESS.2019.2963334

Adaptive Control of Proton Exchange Membrane Fuel Cell Air Supply Systems With Asymmetric Oxygen Excess Ratio Constraints

BYUNG MO KIM, YUN HO CHOI, AND SUNG JIN YOO
School of Electrical and Electronics Engineering, Chung-Ang University, Seoul 06974, South Korea

Corresponding author: Sung Jin Yoo (sjyoo@cau.ac.kr)

This work was supported in part by the National Research Foundation of Korea (NRF) through the Korea Government under Grant NRF-2019R1A2C1004898, and in part by the Human Resources Development, Korea Institute of Energy Technology Evaluation and Planning, through the Korea Government, Ministry of Trade, Industry, and Energy under Grant 20174030201810.

ABSTRACT This paper investigates the oxygen starvation and parasitic loss prevention problem of the adaptive oxygen excess ratio (OER) control system of nonlinear proton exchange membrane fuel cells (PEMFCs). Asymmetric OER constraints are considered to avoid oxygen starvation and parasitic loss in the air supply system of PEMFCs. An approximation-based adaptive control strategy is established to ensure robust regulation of the OER while not violating the OER constraints, regardless of unknown system parameters, nonlinearities, and the abrupt changes of the load current. A dynamic surface design technique using an asymmetric barrier Lyapunov function is employed for a recursive control design. Compared with existing control approaches for uncertain nonlinear air supply systems of PEMFCs, this paper first considers the oxygen starvation and parasitic loss prevention problem for the regulation of optimal OER in the control field of nonlinear PEMFCs. Using the Lyapunov stability theorem, the boundedness of all closed-loop signals and the convergence of the output tracking error to the vicinity of zero are proved.

INDEX TERMS Adaptive control, oxygen excess ratio (OER) constraints, neural networks, proton exchange membrane fuel cells (PEMFCs).

I. INTRODUCTION

Fuel cells are energy conversion devices that transform chemical energy into electrical energy via reactions between hydrogen extracted from gas and oxygen in the air. Fuel cells can provide continuous electricity as long as hydrogen and oxygen are supplied, and their by-products are heat and water. Thus, they are regarded as promising energy devices [1], [2]. Among the various type of fuel cells, proton exchange membrane fuel cells (PEMFCs) have received a considerable amount of attention for both stationary and mobile applications owing to their characteristics such as high energy efficiency, high power density, low operating temperature, and low noise [3], [4]. The structure of PEMFCs is divided into four subsystems: the air supply, the hydrogen flow, the humidity, and the stack temperature systems. Generally, the degree of the stack temperature and humidity cannot change rapidly. Thus, the control problem of these two systems can be decoupled from the rest of the system [5], [6]. On the other hand, compared with simple hydrogen flow systems controlled by an electrical valve, the air supply system controlled by an electrical motor and a compressor exhibits much slower dynamics. Furthermore, the air supply system consumes more electric energy in PEMFCs, diminishing its net output power [7]. Therefore, many researchers have investigated the control problems of the air supply system of PEMFCs [8]–[10]. The control objective of the subsystem is to regulate the oxygen excess ratio (OER), which represents the ratio of consumed amount of oxygen supplied to oxygen reacted to the optimal value for obtaining the maximum efficiency of PEMFC. A linear quadratic regulator [8], a proportional-integral-derivative controller [9], and a passivity-based robust proportional-integral controller [10] were presented for controlling OER of linearized air supply systems. A main issue in controlling OER is to consider

The associate editor coordinating the review of this manuscript and approving it for publication was Zhongyang Fei.

the oxygen starvation phenomenon. Increasing the load current accelerates the amount of used oxygen in the chemical reactions, leading to oxygen starvation. This damages the membrane of the stack and reduces the power response of the fuel cell [11]–[13]. Therefore, there have been attempts to avoid oxygen starvation while regulating OER. In [14], the oxygen starvation protection problem was formulated as a constraint-enforcement problem of OER and a robust nonlinear reference governor approach was presented. In [15], a constrained model predictive control approach was presented to deal with OER constraints. Despite these successful attempts, the load governor and the model predictive controller were based on linearized air supply systems of a certain operating point. However, because the operating point can vary along operating conditions, some researchers have been motivated to develop OER control methods for nonlinear PEMFC systems. In [16], a feedback linearization technique was used to control air supply systems without uncertainties. In [13], a load governor methodology was presented to deal with the oxygen starvation problem of nonlinear PEMFC systems where system uncertainties were not considered. To consider system uncertainties, an adaptive state-observer-based controller was presented in [17] and sliding mode controllers were developed in [18]–[20]. Nevertheless, none of the control approaches [16]–[20] for nonlinear PEMFC systems considered unknown nonlinearities of nonlinear air supply systems. To deal with unknown nonlinearities, an adaptive backstepping control approach was proposed for uncertain nonlinear PEMFC systems where neural networks were employed to estimate completely unknown nonlinearities [21]. Recently, an estimation-based robust control approach was presented for PEMFC systems with unknown nonlinearities [22]. However, the previous control results [16]–[22] for nonlinear air supply systems involve the following restrictions.

R1) In [16]–[22], the constraint problem of OER to avoid oxygen starvation and parasitic loss was not considered for the OER control design of nonlinear air supply systems of PEMFCs. To the best of our knowledge, the oxygen starvation and parasitic loss prevention problem for OER control of uncertain nonlinear air supply systems is still unresolved.

R2) In [21], a class of nonlinear air supply systems with two nonlinearities was considered, and an adaptive neural-network-based controller was designed. However, only one of the nonlinearities was assumed to be unknown and was compensated by a neural network. Furthermore, it was assumed that some system parameters were exactly known, which may be impractical.

R3) In [22], a lumped uncertainty including unknown nonlinear functions and disturbances of air supply systems was estimated, and an estimation-based controller was developed. However, the frequency range of the lumped uncertainty and the system parameter denoting the control coefficient of the input voltage were required for the estimation process.

Some adaptive constraint control approaches have been studied for uncertain constrained nonlinear systems [23]–[26]. In [23], an error transformation approach using multiple prescribed performance bounds was presented for switched nonlinear systems with unknown nonlinearities. In [24], an adaptive constraint control problem of uncertain active suspension systems was considered. Adaptive constraint control problems of uncertain time-delay nonlinear systems with state constraints were investigated in [25] and [26]. In [27] and [28], adaptive fuzzy output-feedback control approaches were studied for uncertain nonlinear systems with state constraints. The visual servoing control problem for a manipulator with visibility constraints was considered in [29]. However, these control designs have not been yet applied to the OER constraint problem of PEMFCs.

Based on these observations, the aim of this study is to propose an adaptive OER control strategy to deal with oxygen starvation and parasitic loss prevention problems of uncertain nonlinear air supply systems of PEMFCs. The nonlinearity denoting the air mass flow from a compressor into a supply manifold is regarded as a completely unknown function and all system parameters are assumed to be unknown. For the controller design, we transform the oxygen starvation and the parasitic loss prevention problem of OER into the OER control problem with asymmetric time-varying constraints. Constructing an asymmetric barrier Lyapunov function [30] and using the dynamic surface design technique [31], an adaptive control scheme is recursively designed where neural network approximators and adaptive tuning laws are derived to compensate for unknown system uncertainties and parameters, respectively. From rigorous stability analysis, it is shown that all the signals of the controlled closed-loop system are semi-globally ultimately uniformly bounded and the control error converges to an adjustable neighborhood of the origin while the asymmetric OER constraints are not violated. Compared with the existing OER control schemes [16]–[22] for uncertain nonlinear air supply systems of PEMFCs, the main contributions of this paper are as follows.

1) Different from the existing control results [16]–[22], this paper considers the constraint problem of OER for avoiding oxygen starvation and parasitic loss of uncertain nonlinear air supply systems. The control problem based on the OER constraints is formulated, and an adaptive control strategy is established in the presence of unknown system nonlinearities and parameters.

2) Compared with the previous adaptive neural-network-based control approach [21] where only a nonlinear function was assumed to be unknown, this paper assumes that all system nonlinearities and parameters are unknown. In addition, the frequency information of uncertainties used in [22] is not required for the proposed control scheme.

The remainder of the paper is structured as follows. In Section II-A, the air supply system of the PEMFC is introduced and some assumptions and lemmas are presented. The background of the OER constraint is given, and the control problem based on the OER constraint is formulated in Section II-B. In Section II-C, some preliminaries for radial basis function neural networks are stated.

TABLE 1. Physical parameters of the fuel-cell system [6].

Symbol	Parameter	Value	SI units
γ	Air specific heat ratio	1.4	-
ϱ	Model reduction constant	25.85×10^{-3}	-
η_{cp}	Compressor efficiency	0.80	-
η_{cm}	Compressor motor mechanical efficiency	0.98	-
A_T	Cathode output throttle area	0.002	m^2
C_D	Cathode output throttle discharge coefficient	0.0124	-
C_p	Air specific heat	1004	$J \cdot (Kg \cdot K)^{-1}$
F	Faraday's constant	96487	$A \cdot s \cdot mol^{-1}$
J_{cp}	Compressor motor inertia	5×10^{-5}	$Kg \cdot m^2$
$k_{ca,in}$	Cathode inlet orifice	0.3629×10^{-5}	$Kg \cdot (s \cdot Pa)^{-1}$
k_t	Motor constant	0.0153	$N \cdot m \cdot A^{-1}$
k_v	Motor constant	0.0153	$V \cdot (rd/s)^{-1}$
M_{O_2}	Molar mass of oxygen	32×10^{-3}	$Kg \cdot mol^{-1}$
M_{N_2}	Molar mass of nitrogen	28×10^{-3}	$Kg \cdot mol^{-1}$
n	Number of cells in fuel-cell stack	381	-
p_{atm}	Atmospheric pressure	101325	Pa
p_{sat}	Saturation pressure	47000	Pa
$\overline{R}$	Universal gas constant	8.14	$J \cdot mol^{-1} \cdot K^{-1}$
R_{cm}	Motor constant	0.82	Ω
T_{st}	Temperature of the fuel-cell stack	353.15	K
T_{atm}	Atmospheric temperature	298.15	K
V_{ca}	Single stack cathode volume	0.01	m^3
ω_{atm}	Humidity ratio of inlet air	0.1885	-
$x_{O_{2,atm}}$	Oxygen mass fraction at cathode inlet	0.233	-

In Sections III-A and III-B, the proposed control design and its stability analysis are presented, respectively. The effectiveness of the proposed controller is validated by the simulation in Section IV. Section V provides the conclusion.

II. PRELIMINARIES AND PROBLEM FORMULATION

A. AIR SUPPLY SYSTEM OF NONLINEAR PEMFC

The air supply model of PEMFC systems having a 75-kW fuel cell stack fed by a 14-kW air turbo compressor was reported in [32]. Based on the fact that the molar mass of the oxygen and nitrogen are nearly the same, this model can be described using a third-order model as follows [5]:

$$\begin{aligned}
\dot{x}_1 &= -l_1 x_1 + l_2 x_2 + c - l_3 \delta, \\
\dot{x}_2 &= l_4 \left[1 + l_5 \left(\frac{x_2}{l_6} \right)^{l_7} - l_5 \right] \\
&\quad \times [\phi(x_2, x_3) - l_8(-x_1 + x_2)], \\
\dot{x}_3 &= -l_9 x_3 - \frac{l_{10}}{x_3} \left[\left(\frac{x_2}{l_6} \right)^{l_7} - 1 \right] \phi(x_2, x_3) + l_{11} u, \qquad (1)
\end{aligned}$$

where x_1 represents the total air pressure inside the cathode comprising the sum of the pressures of oxygen, nitrogen, and vapor, x_2 is the air pressure in the supply manifold, which connected by the air compressor system and the cathode of the PEMFC stack system, x_3 is the rotational speed of the compressor motor, δ is the time-varying load current considered to be a measurable disturbance to the system, and u is the motor input voltage of the compressor. $\phi(x_2, x_3)$ represents the air mass flow from the compressor to the supply manifold, which depends on compressor motor dynamics [2], [32]. Contrary to the existing literature [33] regarding air mass flow $\phi(x_2, x_3)$ as a known nonlinear function, we assume that $\phi(x_2, x_3)$ is a completely unknown nonlinear function. The system parameters l_i, $i = 1, \ldots, 11$ and c are given by

$$\begin{aligned}
&c = \frac{a_3 a_4 p_{sat}}{\varrho}, \; l_1 = a_1 + a_2 + \frac{a_3 a_4}{\varrho}, \; l_2 = a_1 + a_2, \\
&l_3 = \frac{\overline{R} T_{st} n}{4 V_{ca} F}, \; l_4 = \frac{\overline{R} T_{atm}}{J_{cp} \eta_{cp}}, \; l_5 = \frac{1}{\eta_{cp}}, \; l_6 = p_{atm}, \\
&l_7 = \frac{\gamma - 1}{\gamma}, \; l_8 = k_{ca,in}, \; l_9 = \frac{\eta_{cm} k_t k_v}{J_{cp} R_{cm}}, \; l_{10} = \frac{C_p T_{atm}}{J_{cp} \eta_{cp}}, \\
&l_{11} = \frac{\eta_{cm} k_t}{J_{cp} R_{cm}},
\end{aligned}$$

where

$$\begin{aligned}
a_1 &= \frac{\overline{R} T_{st} k_{ca,in}}{M_{O_2} V_{ca}} \left(\frac{x_{O_{2,atm}}}{1 + \omega_{atm}} \right), \\
a_2 &= \frac{\overline{R} T_{st} k_{ca,in}}{M_{N_2} V_{ca}} \left(\frac{1 - x_{O_{2,atm}}}{1 + \omega_{atm}} \right), \; a_3 = \frac{\overline{R} T_{st}}{V_{ca}}, \\
a_4 &= \frac{C_D A_T}{\sqrt{\overline{R} T_{st}}} \gamma^{\frac{1}{2}} \left(\frac{2}{\gamma + 1} \right)^{\frac{\gamma + 1}{2(\gamma - 1)}}.
\end{aligned}$$

Here, the detailed definitions of the used parameters are given in Table 1.

Assumption 1: All system parameters l_i, $i = 1, \ldots, 11$ and c, and the nonlinear function ϕ are unknown.

Assumption 2: The time-varying load current δ and its derivatives $\dot{\delta}$ and $\ddot{\delta}$ are bounded and δ and $\dot{\delta}$ are measurable.

Lemma 1: [34] For any constant $\kappa > 0$ and $\eta \in \mathbb{R}$, the inequality $|\eta| \leq \eta \tanh(\eta/\kappa) + 0.2785\kappa$ holds.

Lemma 2: [30] For any $k_a \in \mathbb{R}$ and $k_b \in \mathbb{R}$, it holds that for $z \in \mathbb{R}$ in the interval $-k_a < z < k_b$,

$$p(z)\log\left(\frac{k_a^2}{k_a^2 - z^2}\right) + (1 - p(z))\log\left(\frac{k_b^2}{k_b^2 - z^2}\right) \leq p(z)\frac{z^2}{k_a^2 - z^2} + (1 - p(z))\frac{z^2}{k_b^2 - z^2} \quad (2)$$

where $p(\bullet)$ is a switching constant defined as

$$p(\bullet) = \begin{cases} 1, & \bullet \leq 0 \\ 0, & \bullet > 0. \end{cases} \quad (3)$$

B. CONTROL PROBLEM BASED ON OER CONSTRAINTS

The OER λ_{O_2} is the ratio of oxygen supplied to the stoichiometric oxygen rate defined as follows:

$$\lambda_{O_2} = \frac{W_{O_2,in}}{W_{O_2,react}} = \frac{\lambda_1(x_2 - x_1)}{\lambda_2 \delta} \quad (4)$$

where $\lambda_1 = k_{ca,in}x_{O_2,atm}/(1 + \omega_{atm})$ and $\lambda_2 = nM_{O_2}/(4F)$. It is well known that the maximum efficiency of the OER corresponds to $\lambda_{O_2}^* = 2$ where $\lambda_{O_2}^*$ is an optimal value [35]. Thus, the OER control objective is regarded as the regulation problem of λ_{O_2} to $\lambda_{O_2}^* = 2$. Moreover, during transients, the OER λ_{O_2} can change abruptly when the load current changes abruptly. When more load current is drawn from the stack, oxygen in the cathode will react instantaneously. Thus, λ_{O_2} drops to a very low value. Then, oxygen starvation is generated when the oxygen flow rate is less than the stoichiometric value (i.e., $\lambda_{O_2} \leq 1$). This damages the fuel cell stack, shortens the cell life limit, and reduces the power response of the cell stock [11]. In the opposite situation, the reduced load current generates the surplus of oxygen in the cathode that leads to parasitic loss (i.e., λ_{O_2} increases quickly to a very high value) [36]. To prevent these phenomena, the constraint problem in the OER control design should be considered.

In this paper, the constrained OER is considered as

$$a \leq \lambda_{O_2} \leq b \quad (5)$$

where $1 < a < 2$ and $2 < b < \infty$ are constants denoting physical constraints of the OER.

Now, let us define the system output y as $y = \lambda_1(x_2 - x_1)$. Then, the regulation problem of λ_{O_2} is transformed into the tracking problem of y to the reference signal $y_r = 2\lambda_2\delta$ and y is required to satisfy the following asymmetric time-varying output constraint:

$$a\lambda_2\delta(t) < y(t) < b\lambda_2\delta(t). \quad (6)$$

By defining the output $y = \lambda_1(x_2 - x_1)$, the constraint (6) is induced from (4) and (5). This implies that the constraint problem of OER λ_{O_2} can be changed to the output constraint problem.

Problem 1: Consider the uncertain air supply system (1) of the PEMFC having OER constraints. Our problem is to design an adaptive control law u ensuring that the system output y tracks the reference signal y_r while the time-varying constraint (5) is not violated.

Remark 1: Different from the existing OER control results for nonlinear air supply systems [16]–[22], this paper firstly considers the OER control problem in the presence of the asymmetric OER constraints, as stated in Problem 1. Thus, the existing results cannot provide a solution to Problem 1.

C. RADIAL BASIS FUNCTION NEURAL NETWORKS

Radial basis function neural networks (RBFNNs) are utilized to approximate unknown nonlinear functions during the control design steps. Based on the universal approximation property of the RBFNN [37], [38], given a continuous real-valued function $Z(\varpi) : \mho_\varpi \mapsto \mathbb{R}$ with a compact set $\mho_\varpi \subset \mathbb{R}^q$, if q is sufficiently large, then there exists an ideal weight vector θ^* such that

$$Z(\varpi) = \theta^{*\top}\xi(\varpi) + \psi(\varpi), \qquad \varpi \in \mho_\varpi \quad (7)$$

where $\varpi = [\varpi_1, \ldots, \varpi_q]^\top \in \mho_\varpi$ denotes the input vector, ψ represents the network reconstruction error, $\theta^* \in \mathbb{R}^r$ with node number $r > 1$ is the optimal weighting vector defined as $\theta^* = \text{argmin}_{\hat{\theta}}[\sup_{\varpi \in \mho_\varpi}|Z(\varpi) - \hat{\theta}^\top\xi(\varpi)|]$; $\hat{\theta}$ is an estimate of θ^*, and $\xi(\varpi) = [\xi_1(\varpi), \xi_2(\varpi), \ldots, \xi_r(\varpi)]^\top \in \mathbb{R}^r$ is a radial basis function. Here, $\xi_i(\varpi)$ are chosen as the following Gaussian functions

$$\xi_i(\varpi) = e^{-\|\varpi - c_i\|^2/\iota^2}, \quad i = 1, \ldots, r \quad (8)$$

where $c_i = [c_{i,1}, \ldots, c_{i,q}]^\top \in \mathbb{R}^q$ is the center of the receptive field and $\iota \in \mathbb{R}$ is the width of the Gaussian functions.

Assumption 3: [37] θ^* and ψ are bounded as $\|\theta^*\| \leq \bar{\theta}$ and $|\psi| \leq \psi^*$, respectively, where $\bar{\theta} > 0$ and $\psi^* > 0$ are unknown constants.

III. MAIN RESULT

A. CONTROLLER DESIGN

The PEMFC air supply systems (1) can be rewritten as

$$\begin{aligned} \dot{x}_1 &= -l_1x_1 + l_2x_2 + c - l_3\delta, \\ \dot{x}_2 &= \Phi_1(x_1, x_2, x_3), \\ \dot{x}_3 &= \Phi_2(x_2, x_3) + l_{11}u, \\ y &= \lambda_1(x_2 - x_1), \end{aligned} \quad (9)$$

where $\Phi_1 = l_4[1 + l_5(x_2/l_6)^{l_7} - l_5][\phi - l_8(-x_1 + x_2)]$ and $\Phi_2 = -l_9x_3 - (l_{10}/x_3)[(x_2/l_6)^{l_7} - 1]\phi$. Note that Φ_1 and Φ_2 are unknown nonlinear functions owing to unknown nonlinearity ϕ and system parameters l_i, $i = 1, \ldots, 11$.

This section focuses on an adaptive controller design for the system (9) with the asymmetric time-varying output constraint (6). The adaptive controller is recursively designed via

the dynamic surface design technique [31]. For the controller design procedure, we define error surfaces as follows:

$$\begin{aligned} z_1 &= y - y_r, \\ z_2 &= x_3 - x_{3r}, \\ \epsilon &= x_{3r} - \alpha, \end{aligned} \tag{10}$$

where z_1 and z_2 are control error surfaces, ϵ is a boundary layer error, α is the virtual control law, and x_{3r} is the filtered virtual control law computed from the following first-order low-pass filter

$$\nu \dot{x}_{3r} + x_{3r} = \alpha, \quad x_{3r}(0) = \alpha(0) \tag{11}$$

with the time constant $\nu > 0$.

Step 1: Consider the first error surface z_1. The time derivative of z_1 along the first and second equations of (9) is given by

$$\begin{aligned} \dot{z}_1 &= \lambda_1(\Phi_1 + l_1 x_1 - l_2 x_2 - c + l_3\delta) - 2\lambda_2\dot{\delta} \\ &= \bar{\Phi}_1 + \lambda_1 l_3 \delta \end{aligned}$$

where $\bar{\Phi}_1(x_1, x_2, x_3, \dot{\delta}) = \lambda_1(\Phi_1 + l_1 x_1 - l_2 x_2 - c) - 2\lambda_2\dot{\delta}$.

From the mean value theorem [39], we represent the function $\bar{\Phi}_1$ as

$$\bar{\Phi}_1(x_1, x_2, \dot{\delta}, x_3) = \bar{\Phi}_1(x_1, x_2, \dot{\delta}, \alpha^*) + g_\chi(x_3 - \alpha^*) \tag{12}$$

where $g_\chi(\bar{x}_\chi) = \partial\bar{\Phi}_1(x_1, x_2, \dot{\delta}, x_3)/\partial x_3|_{x_3 = x_\chi}$ with $x_\chi = \chi x_3 + (1-\chi)\alpha^*$; $\bar{x}_\chi = [x_1, x_2, \dot{\delta}, x_\chi]^\top$, $0 < \chi < 1$ and $\alpha^*(x_1, x_2, \dot{\delta})$ is a smooth function.

Property 1: The function g_χ is unknown, its sign is positive, and there exists an unknown positive constant $g_{\chi 0}$ such that $0 < g_{\chi 0} \le g_\chi$.

Assumption 4: $\dot{g}_\chi$ is bounded as $|\dot{g}_\chi(\cdot)| \le g_{\chi d}$, $\forall \bar{x}_\chi \in \bar{\mathbb{D}}_x \subset \mathbb{R}^4$ where $g_{\chi d} > 0$ is an unknown constant and $\bar{\mathbb{D}}_x$ is a compact region.

Remark 2: The partial derivative of $\bar{\Phi}_1$ with respect to x_3 along (1) and (9) is given by

$$\frac{\partial\bar{\Phi}_1}{\partial x_3} = \lambda_1 l_4(1 + l_5 h)\frac{\partial\phi}{\partial x_3} \tag{13}$$

where $h(x_2) = (x_2/l_6)^{l_7} - 1$. Because $x_2 > l_6 \triangleq p_{atm}$ is always satisfied for system (1) [32], we have $h(x_2) > 0$. On the other hand, the unknown air mass flow nonlinear function $\phi(x_2, x_3)$ is generally adopted by fitting experimental results in the following form [40]

$$\phi = A_1(1 - e^{-\beta(1 - \frac{\Psi}{\Psi_{\max}})})x_3 \tag{14}$$

where $\Psi(x_2, x_3) = A_2 h(x_2)(1/x_3^2)$, A_1, A_2, β, and $\Psi_{\max}$ are positive constants, and the inequality $0 < \Psi(x_2, x_3) < \Psi_{\max}$ holds. Consequently, $\partial\bar{\Phi}_1/\partial x_3$ becomes

$$\begin{aligned} \frac{\partial\bar{\Phi}_1}{\partial x_3} = \lambda_1 l_4(1 + l_5 h)\Bigg[& A_1(1 - e^{-\beta(1 - \frac{\Psi}{\Psi_{\max}})}) \\ & + 2A_1\beta\frac{\Psi}{\Psi_{\max}}e^{-\beta(1 - \frac{\Psi}{\Psi_{\max}})}\Bigg]. \end{aligned} \tag{15}$$

Because $e^{-\beta(1 - \frac{\Psi}{\Psi_{\max}})} < 1$ owing to $\Psi(x_2, x_3) < \Psi_{\max}$, we can conclude that $\partial\bar{\Phi}_1/\partial x_3 > 0$. Therefore, there exists an unknown constant $g_{\chi 0}$ such that $0 < g_{\chi 0} \le g_\chi$.

Based on the implicit function theorem [41], there exists $\alpha^*(x_1, x_2, \dot{\delta})$ such that $\bar{\Phi}_1(x_1, x_2, \dot{\delta}, \alpha^*) = 0$. From this fact and (10), it follows that

$$\dot{z}_1 = g_\chi(z_2 + \epsilon + \alpha - \alpha^*) + \lambda_1 l_3 \delta. \tag{16}$$

Meanwhile, the time-varying output constraint (6) can be transformed into the asymmetric time-varying constraint of z_1 as follows:

$$-k_a(t) < z_1(t) < k_b(t) \tag{17}$$

where $k_a(t) = (2-a)\lambda_2\delta(t)$ and $k_b(t) = (b-2)\lambda_2\delta(t)$ are positive. Thus, the constraint problem of λ_{O_2} can be solved by designing an adaptive control scheme satisfying (17).

Considering (17), an asymmetric barrier Lyapunov function (ABLF) is defined as

$$\begin{aligned} V_{z_1} &= \frac{p(z_1)}{2}\log\frac{k_a^2}{k_a^2 - z_1^2} + \frac{1 - p(z_1)}{2}\log\frac{k_b^2}{k_b^2 - z_1^2} \\ &= \frac{p(z_1)}{2}\log\frac{1}{1 - \varphi_a^2} + \frac{1 - p(z_1)}{2}\log\frac{1}{1 - \varphi_b^2} \end{aligned} \tag{18}$$

where $\varphi_a = z_1/k_a$, $\varphi_b = z_1/k_b$, log denotes the natural logarithm, and $p(z_1)$ is a switching constant defined in Lemma 2. Note that V_{z_1} is zero when z_1 is zero and goes to infinity if $z_1(t)$ goes to the upper time-varying constraint $k_b(t)$ or to the lower time-varying constraint $-k_a(t)$. Thus, (18) is employed to design the adaptive controller satisfying the constraint (17). For simplicity of presentation, we write $p(z_1)$ as p.

The time derivative of V_{z_1} is given by

$$\begin{aligned} \dot{V}_{z_1} &= \frac{p\varphi_a}{1 - \varphi_a^2}\left(\frac{\dot{z}_1}{k_a} - \frac{\dot{k}_a z_1}{k_a^2}\right) + \frac{(1-p)\varphi_b}{1 - \varphi_b^2}\left(\frac{\dot{z}_1}{k_b} - \frac{\dot{k}_b z_1}{k_b^2}\right) \\ &= (p\rho_a + (1-p)\rho_b)\dot{z}_1 - \left(p\rho_a\frac{\dot{k}_a}{k_a} + (1-p)\rho_b\frac{\dot{k}_b}{k_b}\right)z_1 \end{aligned}$$

where $\rho_a = \varphi_a/(k_a(1 - \varphi_a^2))$ and $\rho_b = \varphi_b/(k_b(1 - \varphi_b^2))$. From (3), it holds that $p^2 = p$, $(1-p)^2 = 1 - p$, and $p(1-p) = 0$. Using these properties, we have

$$\begin{aligned} & p\rho_a\frac{\dot{k}_a}{k_a} + (1-p)\rho_b\frac{\dot{k}_b}{k_b} \\ & \qquad = (p\rho_a + (1-p)\rho_b)\left(p\frac{\dot{k}_a}{k_a} + (1-p)\frac{\dot{k}_b}{k_b}\right). \end{aligned}$$

Thus, $\dot{V}_{z_1}$ along (16) becomes

$$\begin{aligned} \dot{V}_{z_1} = (p\rho_a + (1-p)\rho_b)\Bigg(& g_\chi(z_2 + \epsilon + \alpha - \alpha^*) + \lambda_1 l_3\delta \\ & - p\frac{\dot{k}_a z_1}{k_a} - (1-p)\frac{\dot{k}_b z_1}{k_b}\Bigg). \end{aligned} \tag{19}$$

Let $\rho = p\rho_a + (1-p)\rho_b$. Then, using $0 < g_{\chi 0} \le g_\chi$ in Property 1 and $k_a, k_b > 0$, it holds that

$$|\rho\lambda_1 l_3 \delta| \le \frac{g_\chi}{2w_1}\rho^2\lambda_1^2\delta^2 l_3^* + \frac{w_1}{2g_{\chi 0}}, \tag{20}$$

$$-\rho\left(p\frac{\dot{k}_a}{k_a} + (1-p)\frac{\dot{k}_b}{k_b}\right)z_1 \le \frac{g_\chi}{2w_2}\rho^2\left(p\frac{\dot{k}_a^2}{k_a^2} + (1-p)\frac{\dot{k}_b^2}{k_b^2}\right)z_1^2 + \frac{w_2}{2g_{\chi 0}}, \tag{21}$$

where the properties $p(1-p) = 0$, $p^2 = p$, and $(1-p)^2 = 1-p$ are used, $l_3^* = l_3^2$, and w_1 and w_2 are positive constants. Applying (20) and (21) into (19) and using $\dot{k}_a^2/k_a^2 = \dot{k}_b^2/k_b^2 = \dot{\delta}^2/\delta^2$, we have

$$\dot{V}_{z_1} \le \rho g_\chi\left(z_2 + \epsilon + \alpha + Z_1 + \frac{\rho}{2w_1}\lambda_1^2\delta^2 l_3^*\right) + \frac{w_1}{2g_{\chi 0}} + \frac{w_2}{2g_{\chi 0}} \tag{22}$$

where $Z_1(x_1, x_2, \delta, \dot{\delta}) = -\alpha^* + (\rho/(2w_2))(\dot{\delta}^2/\delta^2)z_1^2$. Adding and subtracting $\rho g_\chi(g_{\chi d}/(2g_{\chi 0}^2))z_1$ into (22) yield

$$\dot{V}_{z_1} \le \rho g_\chi\left(z_2 + \epsilon + \alpha + \bar{Z}_1 + \frac{\rho}{2w_1}\lambda_1^2\delta^2 l_3^*\right) - g_\chi\frac{g_{\chi d}}{2g_{\chi 0}^2}\rho z_1 + \frac{w_1}{2g_{\chi 0}} + \frac{w_2}{2g_{\chi 0}} \tag{23}$$

where $\bar{Z}_1(\varpi_1) = Z_1 + (g_{\chi d}/(2g_{\chi 0}^2))z_1$; $\varpi_1 = [x_1, x_2, \delta, \dot{\delta}]^\top$. Using (7), the unknown continuous function $\bar{Z}_1$ is approximated by an RBFNN as follows: $\bar{Z}_1(\varpi_1) = \theta_1^{*\top}\xi_1 + \psi_1$ where $\theta_1^* \in \mathbb{R}^{r_1}$ is an optimal weight vector satisfying $\|\theta_1^*\| \le \bar{\theta}_1$ with a constant $\bar{\theta}_1$, $\xi_1 \in \mathbb{R}^{r_1}$ is a radial basis function vector, $\psi_1 \in \mathbb{R}$ is a reconstruction error satisfying $|\psi_1| \le \psi_1^*$ with a constant ψ_1^*, and r_1 is a node number for the RBFNN. Then, (23) becomes

$$\dot{V}_{z_1} \le \rho g_\chi\left(z_2 + \epsilon + \alpha + \theta_1^{*\top}\xi_1 + \psi_1 + \frac{\rho}{2w_1}\lambda_1^2\delta^2 l_3^*\right) - g_\chi\frac{g_{\chi d}}{2g_{\chi 0}^2}\rho z_1 + \frac{w_1}{2g_{\chi 0}} + \frac{w_2}{2g_{\chi 0}}. \tag{24}$$

From Lemma 1, it holds that

$$\rho g_\chi\psi_1 \le g_\chi|\rho|\psi_1^* \le g_\chi\rho\tanh\left(\frac{\rho}{\kappa_1}\right)\psi_1^* + g_\chi 0.2785\kappa_1\psi_1^* \tag{25}$$

where $\kappa_1 > 0$ is a constant.

Now, a Lyapunov function candidate V_1 is chosen as

$$V_1 = \frac{1}{g_\chi}V_{z_1} + \frac{1}{2}\left(\tilde{\theta}_1^\top\gamma_1^{-1}\tilde{\theta}_1 + \gamma_2^{-1}\tilde{\psi}_1^2 + \gamma_3^{-1}\tilde{l}_3^2\right)$$

where γ_1 is a positive definite matrix, γ_2 and γ_3 are positive parameters, $\tilde{\theta}_1 = \theta_1^* - \hat{\theta}_1$, $\tilde{\psi}_1 = \psi_1^* - \hat{\psi}_1$, and $\tilde{l}_3 = l_3^* - \hat{l}_3$; $\hat{\theta}_1$, $\hat{\psi}_1$, and $\hat{l}_3$ are estimates of θ_1^*, ψ_1^*, and l_3^*, respectively.

Then, the time derivative of V_1 along (24) and (25) is given by

$$\dot{V}_1 \le \rho\left(z_2 + \epsilon + \alpha + \theta_1^{*\top}\xi_1 + \tanh\left(\frac{\rho}{\kappa_1}\right)\psi_1^* + \frac{\rho}{2w_1}\lambda_1^2\delta^2 l_3^*\right) - \frac{\dot{g}_\chi}{g_\chi^2}V_{z_1} - \frac{g_{\chi d}}{2g_{\chi 0}^2}\rho z_1 - \tilde{\theta}_1^\top\gamma_1^{-1}\dot{\hat{\theta}}_1 - \gamma_2^{-1}\tilde{\psi}_1\dot{\hat{\psi}}_1 - \gamma_3^{-1}\tilde{l}_3\dot{\hat{l}}_3 + C_1 \tag{26}$$

where $C_1 = (w_1 + w_2)/(2g_{\chi 0}^2) + 0.2785\kappa_1\psi_1^*$.

The virtual control law α and adaptation laws for $\hat{\theta}_1$, $\hat{\psi}_1$, and $\hat{l}_3$ are chosen as

$$\alpha = -\zeta_1 z_1 - \frac{1}{2w_0}\rho - \hat{\theta}_1^\top\xi_1 - \tanh\left(\frac{\rho}{\kappa_1}\right)\hat{\psi}_1 - \frac{\rho}{2w_1}\lambda_1^2\delta^2\hat{l}_3, \tag{27}$$

$$\dot{\hat{\theta}}_1 = \gamma_1(\rho\xi_1 - \sigma_1\hat{\theta}_1), \tag{28}$$

$$\dot{\hat{\psi}}_1 = \gamma_2\left(\rho\tanh\left(\frac{\rho}{\kappa_1}\right) - \sigma_2\hat{\psi}_1\right), \tag{29}$$

$$\dot{\hat{l}}_3 = \gamma_3\left(\frac{\rho^2}{2w_1}\lambda_1^2\delta^2 - \sigma_3\hat{l}_3\right), \tag{30}$$

where $\zeta_1 > 0$ is a control gain, $w_0 > 0$ is a design parameter, and σ_1, σ_2, $\sigma_3 > 0$ are design parameters for σ-modification [42]. Note that the computational complexity of α is mainly influenced by the structural complexity of the employed neural network $\hat{\theta}_1^\top\xi_1$. Therefore, we can adjust the complexity of α by adjusting the number of nodes r_1 of the neural network.

Substituting (27)–(30) into (26) and using Property 1 and Assumption 4 yields

$$\dot{V}_1 \le -\zeta_1\rho z_1 - \frac{1}{2w_0}\rho^2 + \rho(z_2 + \epsilon) + \frac{g_{\chi d}}{g_{\chi 0}^2}V_{z_1} - \frac{g_{\chi d}}{2g_{\chi 0}^2}\rho z_1 + \sigma_1\tilde{\theta}_1^\top\hat{\theta}_1 + \sigma_2\tilde{\psi}_1\hat{\psi}_1 + \sigma_3\tilde{l}_3\hat{l}_3 + C_1.$$

From Lemma 2, it holds that

$$V_{z_1} \le \frac{1}{2}\left(p\frac{\varphi_a^2}{1-\varphi_a^2} + (1-p)\frac{\varphi_b^2}{1-\varphi_b^2}\right) = \frac{1}{2}\rho z_1.$$

Based on this fact and the inequality $|\rho\epsilon| \le (1/(2w_0))\rho^2 + (w_0/2)\epsilon^2$, we have

$$\dot{V}_1 \le -\zeta_1\rho z_1 + \rho z_2 + \frac{w_0}{2}\epsilon^2 + \sigma_1\tilde{\theta}_1^\top\hat{\theta}_1 + \sigma_2\tilde{\psi}_1\hat{\psi}_1 + \sigma_3\tilde{l}_3\hat{l}_3 + C_1. \tag{31}$$

Step 2: Consider $\dot{x}_3 = \Phi_2(x_2, x_3) + l_{11}u$. Then, the time derivative of a Lyapunov function $V_{z_2} = (1/2)z_2$ is given by

$$\dot{V}_{z_2} = l_{11}z_2(u + Z_2 - l_{11}^*\dot{x}_{3r}) \tag{32}$$

where $l_{11}^* = 1/l_{11}$ and $Z_2(\varpi_2) = l_{11}^*\Phi_2$; $\varpi_2 = [x_2, x_3]^\top$. An RBFNN is employed to approximate Z_2 as $Z_2 = \theta_2^{*\top}\xi_2 + \psi_2$ where $\theta_2^* \in \mathbb{R}^{r_2}$ is an optimal weight vector satisfying $\|\theta_2^*\| \le \bar{\theta}_2$ with a constant $\bar{\theta}_2$, $\xi_2 \in \mathbb{R}^{r_2}$ is a radial basis function

vector, $\psi_2 \in \mathbb{R}$ is a reconstruction error satisfying $|\psi_2| \leq \psi_2^*$ with a constant ψ_2^*, and r_2 is a node number for the RBFNN.

A Lyapunov function candidate V_2 is chosen as

$$V_2 = l_{11}^* V_{z_2} + \frac{1}{2}\left(\tilde{\theta}_2^\top \gamma_4^{-1}\tilde{\theta}_2 + \gamma_5^{-1}\tilde{\psi}_2 + \gamma_6^{-1}\tilde{l}_{11}^2\right) \quad (33)$$

where γ_4 is a positive definite matrix, γ_5 and γ_6 are positive parameters, $\tilde{\theta}_2 = \theta_2^* - \hat{\theta}_2$, $\tilde{\psi}_2 = \psi_2^* - \hat{\psi}_2$, and $\tilde{l}_{11} = l_{11}^* - \hat{l}_{11}$; $\hat{\theta}_2$, $\hat{\psi}_2$, and $\hat{l}_{11}$ are estimates of θ_2^*, ψ_2^*, and l_{11}^*, respectively. By substituting $Z_2 = \theta_2^{*\top}\xi_2 + \psi_2$ into (32) and using the inequality

$$l_{11} z_2 \psi_2 \leq l_{11} z_2 \tanh\left(\frac{z_2}{\kappa_2}\right)\psi_2^* + l_{11} 0.2785 \kappa_2 \psi_2^* \quad (34)$$

with a constant $\kappa_2 > 0$, the time derivative of V_2 is obtained as

$$\dot{V}_2 = z_2\left(u + \theta_2^{*\top}\xi_2 + \tanh\left(\frac{z_2}{\kappa_2}\right)\psi_2^* - l_{11}^*\dot{x}_{3r}\right) + C_2 - \tilde{\theta}_2^\top \gamma_4^{-1}\dot{\hat{\theta}}_2 - \gamma_5^{-1}\tilde{\psi}_2\dot{\hat{\psi}}_2 - \gamma_6^{-1}\tilde{l}_{11}\dot{\hat{l}}_{11} \quad (35)$$

where $C_2 = 0.2785\kappa_2\psi_2^*$.

Now, we propose an actual control law u with adaptation laws for $\hat{\theta}_2$, $\hat{\psi}_2$, $\hat{l}_{11}$, and $\hat{\psi}_2$ as follows:

$$u = -\zeta_2 z_2 - \hat{\theta}_2^\top \xi_2 - \tanh\left(\frac{z_2}{\kappa_2}\right)\hat{\psi}_2 + \hat{l}_{11}\dot{x}_{3r} - \rho, \quad (36)$$

$$\dot{\hat{\theta}}_2 = \gamma_4(z_2\xi_2 - \sigma_4\hat{\theta}_2), \quad (37)$$

$$\dot{\hat{\psi}}_2 = \gamma_5\left(z_2 \tanh\left(\frac{z_2}{\kappa_2}\right) - \sigma_5\hat{\psi}_2\right), \quad (38)$$

$$\dot{\hat{l}}_{11} = \gamma_6(-z_2\dot{x}_{3r} - \sigma_6\hat{l}_{11}), \quad (39)$$

where $\zeta_2 > 0$ is a design parameter, and $\sigma_4 > 0$, $\sigma_5 > 0$ and $\sigma_6 > 0$ are design parameters for σ-modification [42].

Invoking (36)–(39) into (35), we get

$$\dot{V}_2 \leq -\zeta_2 z_2^2 - z_2\rho + \sigma_4\tilde{\theta}_2^\top\hat{\theta}_2 + \sigma_5\tilde{\psi}_2\hat{\psi}_2 + \sigma_6\tilde{l}_{11}\hat{l}_{11} + C_2. \quad (40)$$

Remark 3: In the previous OER control results for uncertain nonlinear PEMFC air supply systems [17]–[22], adaptive or robust controllers were developed to deal with system uncertainties. However, these control schemes cannot prevent the problems of oxygen starvation and parasitic loss caused by the abrupt changes of the load current because constraints on the operating range of OER were not considered in [17]–[22]. On the contrary, we propose an adaptive control scheme that considers the asymmetric constraints on OER of uncertain nonlinear air supply systems (5). Based on the proposed control scheme consisting of (27)–(30) and (36)–(39), the regulation of OER can be achieved without violating the OER constraints and the oxygen starvation and parasitic loss problems are overcome. In addition, in comparison with the existing OER control schemes [17]–[22], the proposed control scheme can be applied to more general PEMFC air supply systems because all system parameters are unknown, as stated in Assumption 1.

Remark 4: For Assumptions 1–4, it is pointed out that

(i) Assumption 1 is reasonable because the system parameters l_i, $i = 1, \ldots, 11$ and c cannot be exactly known in practical engineering systems and the air mass flow ϕ is generally adopted by fitting experimental results [40]. Thus, l_i, c, and ϕ are assumed to be unknown.

(ii) As reported in [21] and [32], the load current δ is measurable for the regulation problem of OER, and δ and its derivatives are bounded signals because of the physical meaning of δ. Thus, Assumption 2 is a reasonable assumption.

(iii) Owing to the function approximation property of RBFNN [37], [38], the optimal weights and reconstruction error of RBFNN are bounded. In this paper, their bounds are assumed to be unknown. Thus, Assumption 3 is a general assumption in the neural network control field.

(iv) Assumption 4 means that the time derivative of g_χ is bounded in the compact set $\overline{\mathbb{D}}_x \subset \mathbb{R}^4$. Here, g_χ is well-defined function, as discussed in Remark 2, and is differentiable because of $x_2 > l_6$ and $x_3 > 0$. Therefore, Assumption 4 is reasonable.

B. STABILITY ANALYSIS

The stability of the closed-loop system is analyzed in this section. The dynamics of the boundary layer error is given by

$$\dot{\epsilon} = -\frac{\epsilon}{\nu} + B(z_1, z_2, \epsilon, \hat{\theta}_1, \hat{\psi}_1, \hat{l}_3, \bar{\delta}) \quad (41)$$

where $\bar{\delta} = [\delta, \dot{\delta}, \ddot{\delta}]^\top$ and

$$B = \zeta_1\dot{z}_1 + \frac{\dot{\rho}}{2w_0} + \dot{\hat{\theta}}_1^\top\xi_1 + \hat{\theta}_1^\top\dot{\xi}_1 + \operatorname{sech}^2\left(\frac{\rho}{\kappa_1}\right)\frac{\dot{\rho}}{\kappa_1}\hat{\psi}_1 + \tanh\left(\frac{\rho}{\kappa_1}\right)\dot{\psi}_1 + \frac{\dot{\rho}}{2w_1}\lambda_1^2\delta^2\hat{l}_3 + \frac{\rho}{w_1}\lambda_1^2\delta\dot{\delta}\hat{l}_3 + \frac{\rho}{2w_1}\lambda_1^2\delta^2\dot{\hat{l}}_3.$$

Consider the total Lyapunov function candidate V

$$V = V_1 + V_2 + \frac{1}{2}\epsilon^2. \quad (42)$$

Theorem 1: Consider the PEMFC air supply system (1) with the asymmetric OER constraint (5) controlled by the proposed adaptive controller consisting of (27)–(30) and (36)–(39) under Assumptions 1–4. For any initial conditions satisfying $V(0) \leq \mu$ with a constant $\mu > 0$ and $a\lambda_2\delta(0) < y(0) < b\lambda_2\delta(0)$, all the signals in the closed-loop system are uniformly bounded and the tracking error z_1 converges to an adjustable neighborhood of the origin while the OER constraints are guaranteed.

Proof: From (31), (40), and (41), the time derivative of V is represented by

$$\begin{aligned}\dot{V} \leq & -\zeta_1\rho z_1 - \zeta_2 z_2^2 - \frac{1}{\nu}\epsilon^2 + \frac{w_0}{2}\epsilon^2 + \epsilon B - \frac{\sigma_1}{2}\|\tilde{\theta}_1\|^2 \\ & - \frac{\sigma_2}{2}\tilde{\psi}_1^2 - \frac{\sigma_3}{2}\tilde{l}_3^2 - \frac{\sigma_4}{2}\|\tilde{\theta}_2\|^2 - \frac{\sigma_5}{2}\tilde{\psi}_2^2 - \frac{\sigma_6}{2}\tilde{l}_{11}^2 + \frac{\sigma_1}{2}\bar{\theta}_1^2 \\ & + \frac{\sigma_2}{2}(\psi_1^*)^2 + \frac{\sigma_3}{2}(l_3^*)^2 + \frac{\sigma_4}{2}\bar{\theta}_2^2 + \frac{\sigma_5}{2}(\psi_2^*)^2 + \frac{\sigma_6}{2}(l_{11}^*)^2 \\ & + C_1 + C_2. \end{aligned} \tag{43}$$

Consider the set $\Xi := \{(1/g_\chi)(p\log(k_a^2/(k_a^2 - z_1^2)) + (1-p)\log(k_b^2/(k_b^2 - z_1^2))) + \tilde{\theta}_1^\top \gamma_1^{-1}\tilde{\theta}_1 + \gamma_2^{-1}\tilde{\psi}_1^2 + \gamma_3^{-1}\tilde{l}_3^2 + \tilde{\theta}_2^\top \gamma_4^{-1}\tilde{\theta}_2 + \gamma_5^{-1}\tilde{\psi}_1^2 + \gamma_6^{-1}\tilde{l}_{11}^2 + \epsilon^2 \leq 2\mu\}$ and $D = \{(\delta, \dot{\delta}, \ddot{\delta}) | \delta^2 + \dot{\delta}^2 + \ddot{\delta}^2 \leq \mu_r\}$ with a constant $\mu_r > 0$. Because $\Xi \times D$ is compact in $\mathbb{R}^{6+r_1+r_2+3}$, there exists a constant $M > 0$ such that $|B| \leq M$ on $\Xi \times D$.

Using the following inequality $(B^2/(2\,w_3))\epsilon^2 + w_3/2$ with a positive constant w_3 and the property $-\zeta_1\rho z_1 \leq -2\zeta_1 V_{z_1}$ from Lemma 2 and choosing $1/\nu = w_0/2 + M^2/(2w_3) + \bar{\nu}$ with a constant $\bar{\nu} > 0$, (43) becomes

$$\begin{aligned}\dot{V} \leq & -2\zeta_1 V_{z_1} - \zeta_2 z_2^2 - \bar{\nu}\epsilon^2 - \frac{\sigma_1}{2}\|\tilde{\theta}_1\|^2 - \frac{\sigma_2}{2}\tilde{\psi}_1^2 \\ & - \frac{\sigma_3}{2}\tilde{l}_3^2 - \frac{\sigma_4}{2}\|\tilde{\theta}_2\|^2 - \frac{\sigma_5}{2}\tilde{\psi}_2^2 - \frac{\sigma_6}{2}\tilde{l}_{11}^2 \\ & - \left(1 - \frac{B^2}{M^2}\right)\frac{M^2\epsilon^2}{2w_3} + C. \end{aligned} \tag{44}$$

On $V = \mu$, (44) becomes $\dot{V} \leq -LV + C$ where $L = \min\{2\zeta_1 g_{\chi 0}, 2\zeta_2, 2\bar{\nu}, \sigma_1/(\lambda_{\max}(\gamma_1^{-1})), \sigma_2\gamma_2, \sigma_3\gamma_3, \sigma_4/(\lambda_{\max}(\gamma_4^{-1})), \sigma_5\gamma_5, \sigma_6\gamma_6\}$. When $L > C/\mu$, $\dot{V} < 0$ on $V = \mu$. Thus, it holds that $V \leq \mu$ is an invariant set which implies that V_{z_1} is bounded. From the boundedness of V_{z_1}, it is induced that $|\varphi_a| < 1$ for $z_1 \leq 0$ and $|\varphi_b| < 1$ for $z_1 > 0$. Owing to $\varphi_a = z_1/k_a$ and $\varphi_b = z_1/k_b$, the inequality $-k_a(t) < z_1(t) < k_b(t)$ holds for all $t \geq 0$, which leads to $a < \lambda_{O_2}(t) < b$, $\forall t \geq 0$. Thus, all signals of the closed-loop system are semi-globally uniformly ultimately bounded while ensuring the OER constraints. From the boundedness of all signals and Assumption 2, there exists a constant $\bar{g}_\chi$ such that $|g_\chi| \leq \bar{g}_\chi$. In addition, integrating $\dot{V} \leq -LV + C$ with respect to times yields $\frac{1}{\bar{g}_\chi}V_{z_1} \leq V(t) \leq e^{-Lt}V(0) + (C/L)(1 - e^{-Lt})$. After some manipulations, it follows that

$$|\varphi_j| \leq \sqrt{1 - e^{-2\bar{g}_\chi[V(0)e^{-Lt} + (C/L)(1-e^{-Lt})]}}$$

where $j = a, b$. Thus, $|\varphi_j| \leq \sqrt{1 - e^{-(2\bar{g}_\chi(C/L))}}$ as $t \to \infty$. From $\varphi_a = z_1/k_a$ and $\varphi_b = z_1/k_b$, the tracking error z_1 can be arbitrarily small by adjusting design parameters (see Remark 5). ■

Remark 5: The design parameters of the proposed adaptive controller can be chosen via the proof of Theorem 1. The guidelines for selecting design parameters are provided as follows:

1) Increasing ζ_1 and ζ_2 and decreasing ν help to increase L, which subsequently reduces the bound $\sqrt{1 - e^{-2\bar{g}_\chi(C/L)}}$ of ψ_j where $j = a, b$. Thus, the tracking error z_1 can be reduced.

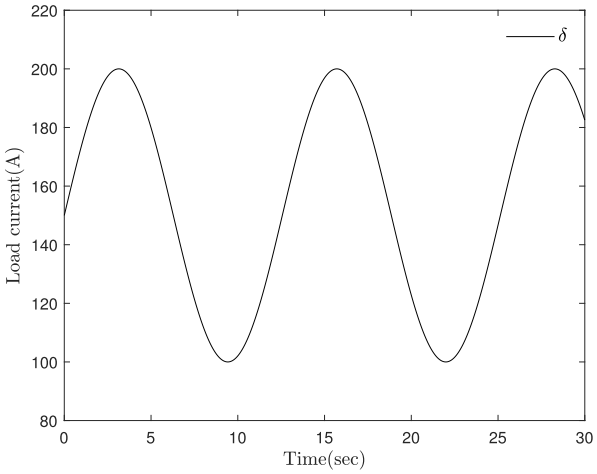

FIGURE 1. Load current for case 1.

2) Decreasing w_i, κ_1, and κ_2 helps to reduce C which leads to reduce the bound $\sqrt{1 - e^{-2\bar{g}_\chi(C/L)}}$ of ψ_j. This helps to reduce the tracking error z_1.

3) Fixing σ_i as small constants and increasing γ_i help to increase the tuning speed of the adaptive parameters θ_1, θ_2, ψ_1, ψ_2, l_3, and l_{11}.

IV. SIMULATION RESULTS

To illustrate the effectiveness of the proposed control scheme, we consider the PEMFC air supply system (1) whose system parameters are given in Table 1. In addition, compared with an adaptive controller designed without using ABLF, the constraint satisfaction of the proposed ABLF-based controller is shown where the adaptive controller designed without using ABLF is designed by redefining V_{z_1} in (18) as $V_{z_1} = z_1^2$. We simulate two cases according to the type of the load current.

Case 1: In this case, we consider the time-varying load current $\delta(t) = 150 + 50\sin(0.5t)$, as displayed in Fig. 1. The parameters for the asymmetric constraints on the output $y = \lambda_1(x_2 - x_1)$ with $\lambda_1 = 7.11 \times 10^{-7}$ are set to $a = 1.8$ and $b = 2.3$. The reference signal is $y_r(t) = 2\lambda_2\delta(t)$ with $\lambda_2 = 3.16 \times 10^{-5}$. The initial values of the state variables are chosen as $x_1(0) = 1.6 \times 10^5$, $x_2(0) = 1.75 \times 10^5$, and $x_3(0) = 6.7 \times 10^3$. Then, we choose the design parameters of the proposed control scheme as $\zeta_1 = 1$, $\zeta_2 = 1$, $\nu = 0.01$, $w_0 = w_1 = 5$, $\kappa_1 = \kappa_2 = 1$, $\gamma_1 = \text{diag}[1]$, $\gamma_2 = 0.1$, $\gamma_3 = 10^5$, $\gamma_4 = \text{diag}[0.01]$, $\gamma_5 = 0.05$, $\gamma_6 = 10^{-7}$, $\sigma_1 = 10^{-3}$, $\sigma_2 = 2$, $\sigma_3 = 3.5 \times 10^{-10}$, $\sigma_4 = 1$, $\sigma_5 = 0.1$, and $\sigma_6 = 1$.

The output tracking results of the proposed ABLF-based controller and those of the controller designed without using ABLF are compared in Fig. 2. Fig. 3 shows the OER regulation results of the proposed controller and the controller designed without using ABLF. While the output response of the proposed ABLF-based control system remains within the asymmetric constraints (see Fig. 2(a)), the output response of the control system designed without using ABLF violates the asymmetric constraints in the transient response

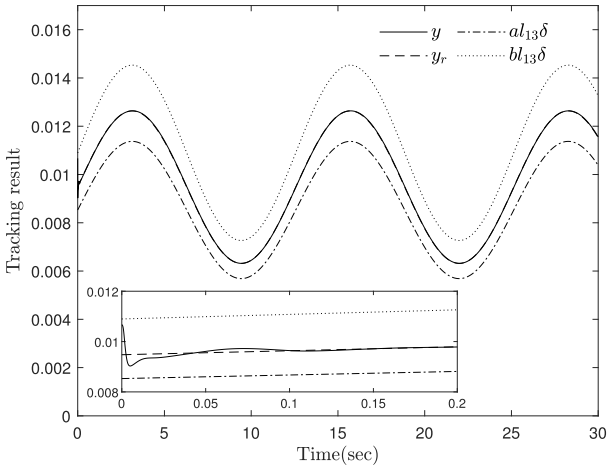

(a)

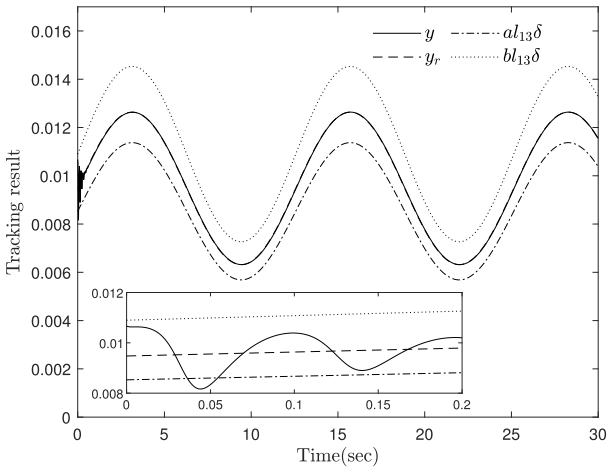

(b)

FIGURE 2. Comparison of the tracking results for case 1 (a) y, y_r, and constraints of the proposed control system (b) y, y_r, and constraints of the control system designed without using ABLF.

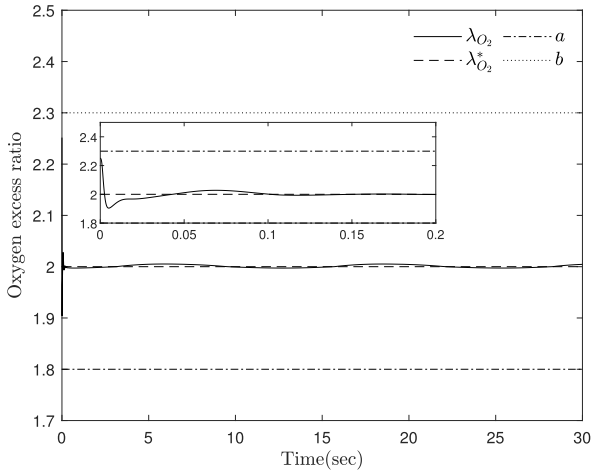

(a)

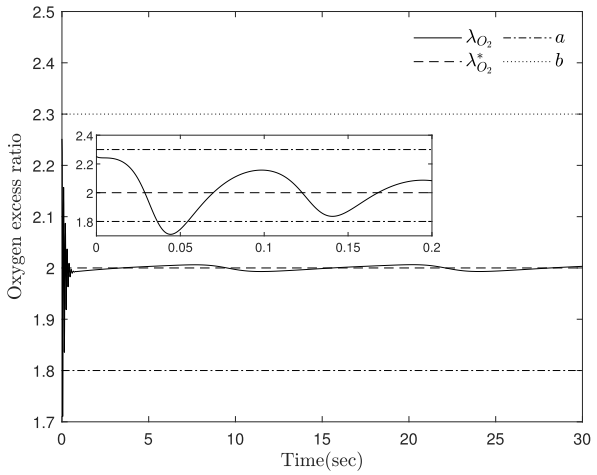

(b)

FIGURE 3. Comparison of the OER regulation for Case 1 (a) λ_{O_2}, $\lambda^*_{O_2}$, and constraints of the proposed control system (b) λ_{O_2}, $\lambda^*_{O_2}$, and constraints of the control system designed without using ABLF.

(see Fig. 2(b)). These results are also observed in Fig. 3 where the OER response of the control system designed without using ABLF gets out of the lower bound b in the transient response (see Fig. 3(b)). This means that the control system designed without using ABLF may experience oxygen starvation. Thus, both the OER regulation and the prevention of oxygen starvation and parasitic loss can be achieved with the proposed control approach. Fig. 4 displays the control input voltage u of the proposed control scheme. It is shown that the control input (i.e, motor compressor voltage) consistently changes because of the time-varying load current δ. Fig. 5 shows the RBFNN outputs and the adaptive parameters of the proposed control scheme where the RBFNN outputs $\hat{\theta}_1^\top \xi_1$ and $\hat{\theta}_2^\top \xi_2$ compensate for the nonlinearities $\bar{Z}_1$ and Z_2, respectively.

Case 2: We set to $a = 1.6$ and $b = 2.5$ for the constraints on y and the load current δ is defined as constant values between 200A to 310A, as illustrated in Fig. 6. The initial values of

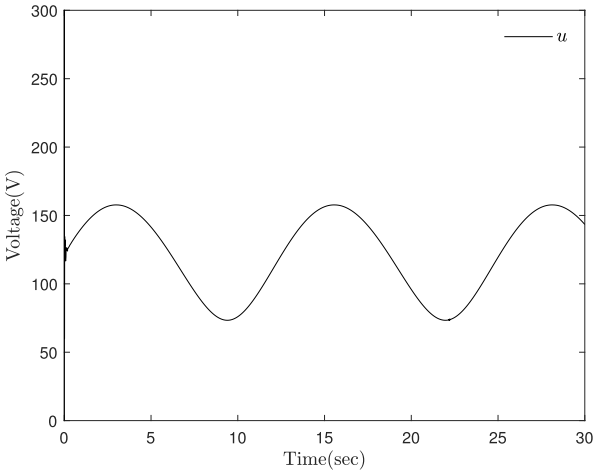

FIGURE 4. Control input voltage of the proposed control system for case 1.

the state variables are chosen as $x_1(0) = 1.6 \times 10^5$, $x_2(0) = 1.81 \times 10^5$, and $x_3(0) = 6.7 \times 10^3$. The design parameters

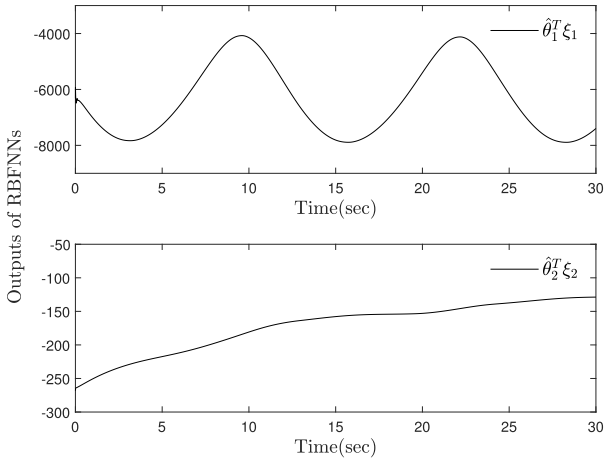

(a)

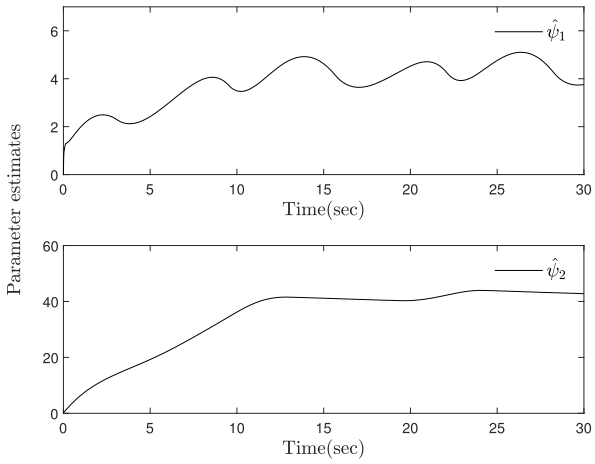

(b)

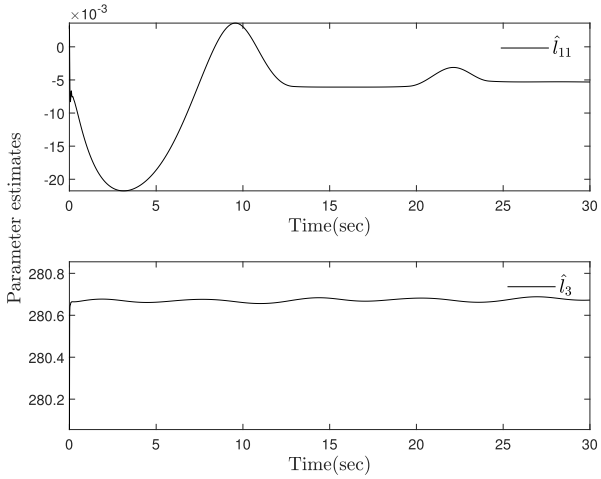

(c)

FIGURE 5. RBFNN outputs and adaptive parameters of the proposed control system for Case 1 (a) $\hat{\theta}_1^T\xi_1$ and $\hat{\theta}_2^T\xi_2$ (b) $\hat{\psi}_1$ and $\hat{\psi}_2$ (c) $\hat{l}_3$ and $\hat{l}_{11}$.

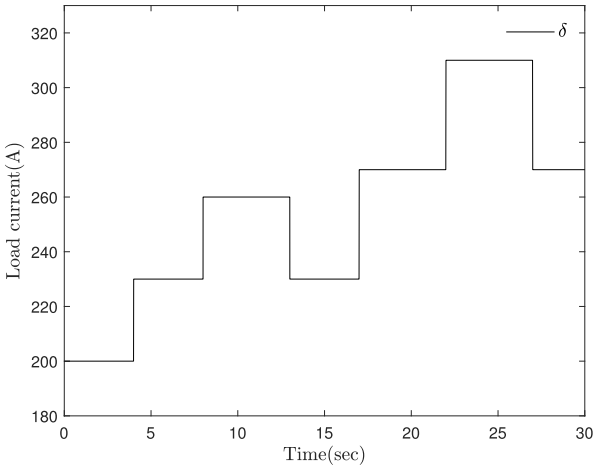

FIGURE 6. Load current for case 2.

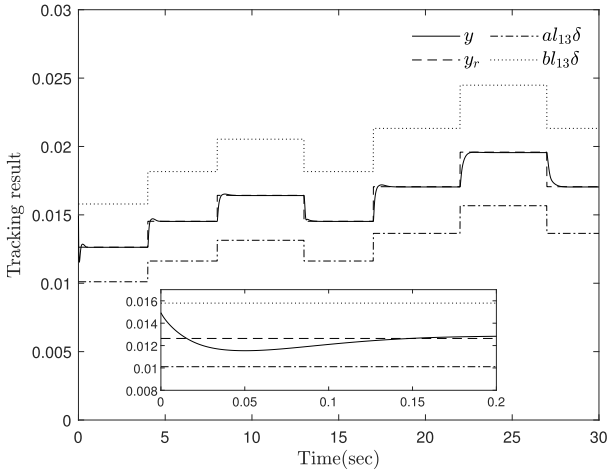

(a)

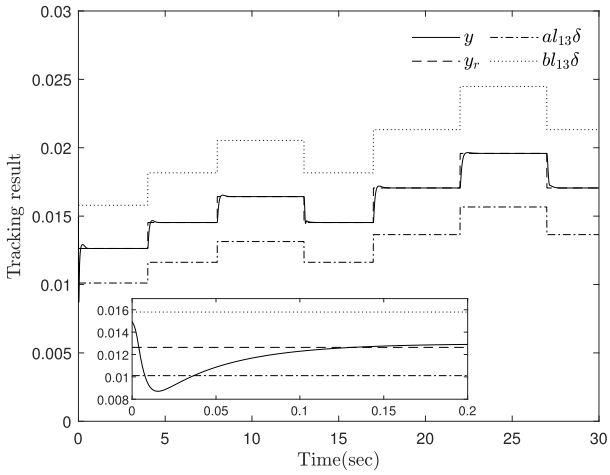

(b)

FIGURE 7. Comparison of the tracking results for Case 2 (a) y, y_r, and constraints of the proposed control system (b) y, y_r, and constraints of the control system designed without using ABLF.

are chosen as $\zeta_1 = 2$, $\zeta_2 = 2$, $\nu = 0.01$, $w_0 = w_1 = 1$, $\kappa_1 = \kappa_2 = 1$, $\gamma_1 = \text{diag}[15]$, $\gamma_2 = 0.5$, $\gamma_3 = 10^4$, $\gamma_4 = \text{diag}[1]$, $\gamma_5 = 0.1$, $\gamma_6 = 10^{-7}$, $\sigma_i = 10^{-3}$, $\sigma_2 = 1$, $\sigma_3 = 4 \times 10^{-8}$, and $\sigma_5 = 0.2$ where $i = 1, 4, 6$.

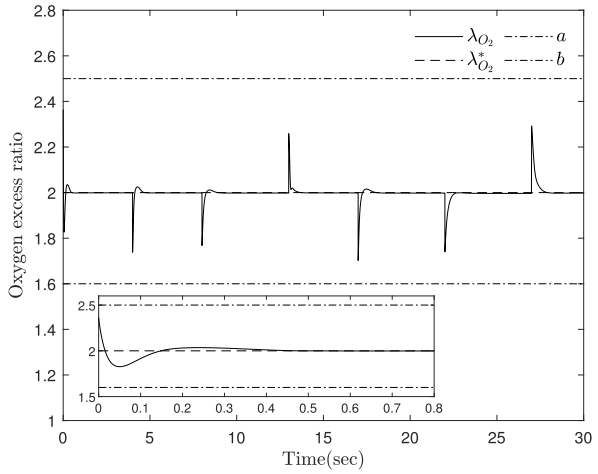

(a)

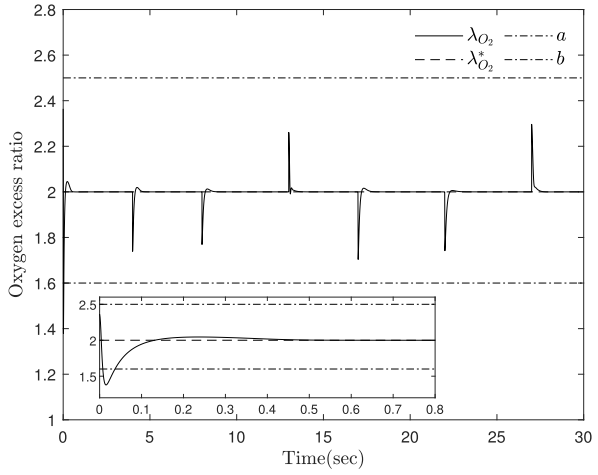

(b)

FIGURE 8. Comparison of the OER regulation for case 2 (a) λ_{O_2}, $\lambda^*_{O_2}$, and constraints of the proposed control system (b) λ_{O_2}, $\lambda^*_{O_2}$, and constraints of the control system designed without using ABLF.

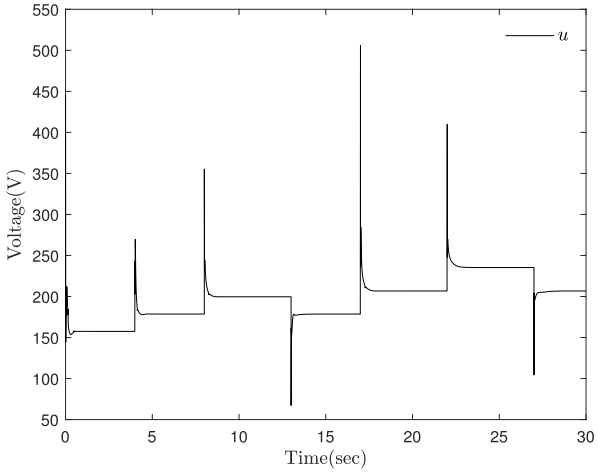

FIGURE 9. Control input voltage of the proposed control system for case 2.

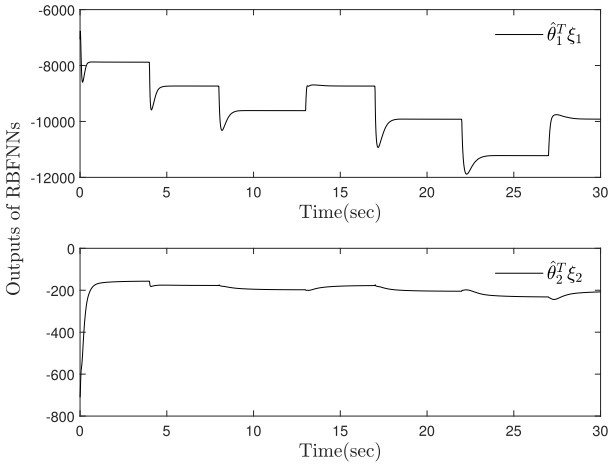

(a)

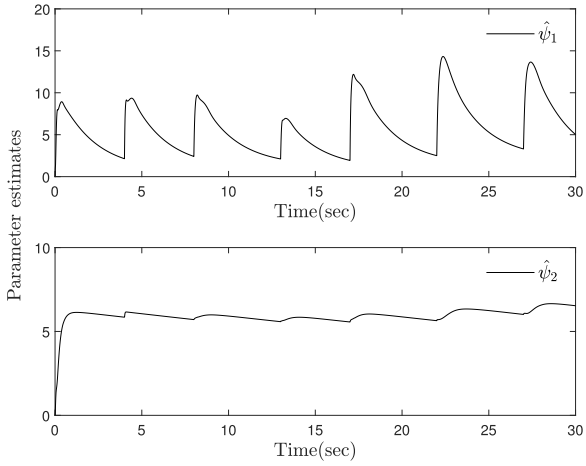

(b)

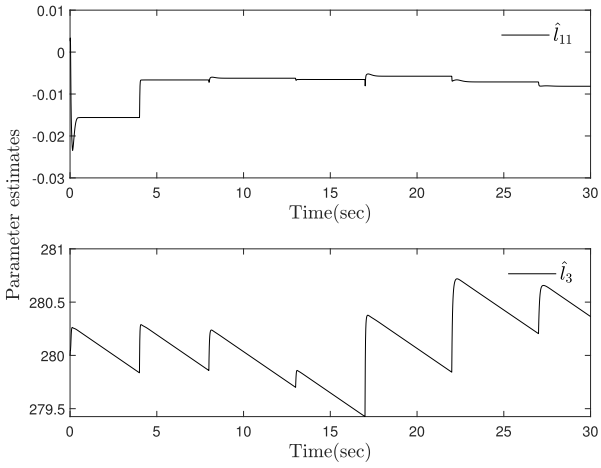

(c)

FIGURE 10. RBFNN outputs and adaptive parameters of the proposed control system for Case 2 (a) $\hat{\theta}_1^T\xi_1$ and $\hat{\theta}_2^T\xi_2$ (b) $\hat{\psi}_1$ and $\hat{\psi}_2$ (c) $\hat{l}_3$ and $\hat{l}_{11}$.

In Figs. 7 and 8, the output tracking and OER regulation results of the proposed ABLF-based controller and the controller designed without using ABLF are compared. Figs. 7(b) and 8(b) show that the controller designed without

using ABLF cannot ensure OER constraint satisfaction while regulating λ_{O_2} to $\lambda^*_{O_2}$. However, the OER response λ_{O_2} of the proposed control system is confined within the asymmetric constraints although the load current δ changes abruptly and the air supply system (1) includes unknown system parameters and nonlinearities. Fig. 9 shows the control input u of the proposed control system where u varies as δ varies. Fig. 10 depicts the RBFNN outputs and the adaptive parameters.

V. CONCLUSION

This paper has presented an adaptive OER control strategy to prevent oxygen starvation and parasitic loss of uncertain nonlinear air supply systems of PEMFCs. An approximation-based adaptive controller using ABLF has been designed to ensure OER regulation within OER constraints where neural network approximators and adaptation parameters were employed to compensate for system uncertainties. The concerned design problem has been the first trial in the OER control field of nonlinear air supply systems of PEMFCs. The stability and OER constraint satisfaction of the resulting closed-loop system have been analyzed via the Lyapunov stability theorem. The simulation results have demonstrated the effectiveness of the proposed control scheme against changes in the load current and system uncertainties.

REFERENCES

[1] I. M. M. Saleh, R. Ali, and H. Zhang, "Simplified mathematical model of proton exchange membrane fuel cell based on horizon fuel cell stack," *J. Mod. Power Syst. Clean Energy*, vol. 4, no. 4, pp. 668–679, Apr. 2016.
[2] M. Grujicic, K. M. Chittajallu, E. H. Law, and J. T. Pukrushpan, "Model-based control strategies in the dynamic interaction of air supply and fuel cell," *Inst. Mech. Eng., A, J. Power Energy*, vol. 218, no. 7, pp. 487–499, Nov. 2004.
[3] D. Feroldi and M. S. Basualdo, *PEM Fuel Cells With Bio-Ethanol Processor Systems*. London, U.K.: Springer-Verlag, 2012.
[4] O. Z. Sharaf and M. F. Orhan, "An overview of fuel cell technology: Fundamentals and applications," *Renew. Sustain. Energy Rev.*, vol. 32, pp. 810–853, Apr. 2014.
[5] R. J. Talj, D. Hissel, R. Ortega, M. Becherif, and M. Hilairet, "Experimental validation of a PEM fuel–cell reduced–order model and a Moto–compressor higher order sliding–mode control," *IEEE Trans. Ind. Electron.*, vol. 57, no. 6, pp. 1906–1913, Jun. 2010.
[6] R. J. Talj, R. Ortega, and M. Hilairet, "A controller tuning methodology for the air supply system of a PEM fuel cell system with guaranteed stability properties," *Int. J. Control.*, vol. 82, no. 9, pp. 1706–1719, Sep. 2009.
[7] A. Vahidi, A. Stefanopoulou, and H. Peng, "Current management in a hybrid fuel cell power system: A model–predictive control approach," *IEEE Trans. Control Syst. Technol.*, vol. 14, no. 6, pp. 1047–1057, Nov. 2006.
[8] J.-W. Ahn and S.-Y. Choe, "Coolant controls of a PEM fuel cell system," *J. Power Sources*, vol. 179, no. 1, pp. 252–264, Apr. 2008.
[9] A. Niknezhadi, M. Allué-Fantova, C. Kunusch, and C. Ocampo-Martínez, "Design and implementation of LQR/LQG strategies for oxygen stoichiometry control in PEM fuel cells based systems," *J. Power Sources*, vol. 196, no. 9, pp. 4277–4282, May 2011.
[10] R. Talj, R. Ortega, and A. Astolfi, "Passivity and robust PI control of the air supply system of a PEM fuel cell model," *Automatica*, vol. 47, no. 12, pp. 2554–2561, Dec. 2011.
[11] E. A. M. Ali and A. Abudhahir, "A survey of the relevance of control systems for PEM fuel cells," in *Proc. Int. Conf. Comput., Commun. Elect. Technol. (ICCCET)*, Mar. 2011, Tamilnadu, India, pp. 18–19.
[12] A. Vahidi, I. Kolmanovsky, and A. Stefanopoulou, "Constraint handling in a fuel cell system: A fast reference governor approach," *IEEE Trans. Control Syst. Technol.*, vol. 15, no. 1, pp. 86–98, Jan. 2007.
[13] S. Laghrouche, I. Matraji, F. S. Ahmed, S. Jemei, and M. Wack, "Load governor based on constrained extremum seeking for PEM fuel cell oxygen starvation and compressor surge protection," *Int. J. Hydrogen Energy*, vol. 38, no. 33, pp. 14314–14322, Nov. 2013.
[14] J. Sun and I. Kolmanovsky, "Load governor for fuel cell oxygen starvation protection: A robust nonlinear reference governor approach," *IEEE Trans. Control Syst. Technol.*, vol. 13, no. 6, pp. 911–920, Nov. 2005.
[15] M. Abdullah and M. Idres, "Constrained model predictive control of proton exchange membrane fuel cell," *J. Mech. Sci. Technol.*, vol. 28, no. 9, pp. 3855–3862, Sep. 2014.
[16] J. Chen, Z. Liu, F. Wang, Q. Ouyang, and H. Su, "Optimal oxygen excess ratio control for PEM fuel cells," *IEEE Trans. Control Syst. Technol.*, vol. 26, no. 5, pp. 1711–1721, Sep. 2018.
[17] K. Sankar and A. K. Jana, "Dynamics and estimator–based nonlinear control of a PEM fuel cell," *IEEE Trans. Control Syst. Technol.*, vol. 26, no. 3, pp. 1124–1131, May 2018.
[18] J. Liu, Y. Gao, X. Su, M. Wack, and L. Wu, "Disturbance-observer-based control for air management of PEM fuel cell systems via sliding mode technique," *IEEE Trans. Control Syst. Technol.*, vol. 27, no. 3, pp. 1129–1138, May 2019.
[19] A. Pilloni, A. Pisano, and E. Usai, "Observer–based air excess ratio control of a PEM fuel cell system via high–order sliding mode," *IEEE Trans. Ind. Electron.*, vol. 62, no. 8, pp. 5236–5246, Aug. 2015.
[20] H. Deng, Q. Li, Y. Cui, Y. Zhu, and W. Chen, "Nonlinear controller design based on cascade adaptive sliding mode control for PEM fuel cell air supply systems," *Int. J. Hydrogen Energy*, vol. 44, no. 35, pp. 19357–19369, Jul. 2019.
[21] P. Li, J. Chen, T. Cai, and B. Zhang, "Adaptive control of air delivery system for PEM fuel cell using backstepping," in *Proc. 8th Asian Control Conf.*, Kaohsiung, Taiwan, May 2011, pp. 1282–1287.
[22] Z. Liu, J. Chen, H. Chen, and C. Yan, "Air supply regulation for PEMFC systems based on uncertainty and disturbance estimation," *Int. J. Hydrogen Energy*, vol. 43, no. 25, pp. 11559–11567, Jun. 2018.
[23] L. Liu, Y.-J. Liu, and S. Tong, "Fuzzy–based multierror constraint control for switched nonlinear systems and its applications," *IEEE Trans. Fuzzy Syst.*, vol. 27, no. 8, pp. 1519–1531, Aug. 2019.
[24] Y. J. Liu, Q. Zeng, C. L. Chen, and L. Liu, "Actuator failure compensation-based adaptive control of active suspension systems with prescribed performance," *IEEE Trans. Ind Electron.*, to be published, doi: 10.1109/TIE.2019.2937037.
[25] D.-P. Li, Y.-J. Liu, S. Tong, C. L. P. Chen, and D.-J. Li, "Neural networks–based adaptive control for nonlinear state constrained systems with input delay," *IEEE Trans. Cybern.*, vol. 49, no. 4, pp. 1249–1258, Apr. 2019.
[26] D. Li, C. L. P. Chen, Y.-J. Liu, and S. Tong, "Neural network controller design for a class of nonlinear delayed systems with time–varying full–state constraints," *IEEE Trans. Neural Netw. Learn. Syst.*, vol. 30, no. 9, pp. 2625–2636, Sep. 2019.
[27] Y.-J. Liu, M. Gong, S. Tong, C. L. P. Chen, and D.-J. Li, "Adaptive fuzzy output feedback control for a class of nonlinear systems with full state constraints," *IEEE Trans. Fuzzy Syst.*, vol. 26, no. 5, pp. 2607–2617, Oct. 2018.
[28] Y.-J. Liu, M. Gong, L. Liu, S. Tong, and C. L. P. Chen, "Fuzzy observer constraint based on adaptive control for uncertain nonlinear MIMO systems with time-varying state constraints," *IEEE Trans. Fuzzy Syst.*, to be published, doi: 10.1109/TCYB.2019.2933700.
[29] Y. Zhang, C. Hua, Y. Li, and X. Guan, "Adaptive neural networks-based visual servoing control for manipulator with visibility constraint and dead-zone input," *Neurocomputing*, vol. 332, pp. 44–55, Mar. 2019.
[30] Z. Zhao, W. He, and S. S. Ge, "Adaptive neural network control of a fully actuated marine surface vessel with multiple output constraints," *IEEE Trans. Control Syst. Technol.*, vol. 22, no. 4, pp. 1536–1543, Jul. 2014.
[31] D. Swaroop, J. K. Hedrick, P. P. Yip, and J. C. Gerdes, "Dynamic surface control for a class of nonlinear systems," *IEEE Trans. Autom. Control*, vol. 45, no. 10, pp. 1893–1899, Oct. 2000.
[32] J. T. Pukrushpan, A. G. Stefanopoulou, and H. Peng, *Control of Fuel Cell Power Systems: Principles, Modeling, Analysis and Feedback Design*. London, U.K.: Springer-Verlag, 2004.
[33] J. T. Pukrushpan, A. G. Stefanopoulou, and H. Peng, "Control of fuel cell breathing," *IEEE Control Syst.*, vol. 24, no. 2, pp. 30–46, Apr. 2004.
[34] M. Polycarpou, "Stable adaptive neural control scheme for nonlinear systems," *IEEE Trans. Autom. Control*, vol. 41, no. 3, pp. 447–451, Mar. 1996.
[35] J. T. Pukrushpan, *Modeling and Control of Fuel Cell Systems and Fuel Processors*. Ann Arbor, MN, USA: Univ. of Michigan, 2003.

[36] V. Shishodia, *Enhanced Control Performance and Application to Fuel Cell Systems*. Gainesville, FL, USA: Univ. of Florida, 2008.
[37] C. Wang, D. J. Hill, S. Ge, and G. Chen, "An ISS-modular approach for adaptive neural control of pure-feedback systems," *Automatica*, vol. 42, no. 5, pp. 723–731, May 2006.
[38] A. J. Kurdila, F. J. Narcowich, and J. D. Ward, "Persistency of excitation in identification using radial basis function approximants," *SIAM J. Control Optim.*, vol. 33, no. 2, pp. 625–642, Mar. 1995.
[39] H. Jeffreys, *Methods of Mathematical Physics*. Cambridge, U.K.: Cambridge Univ. Press, 1988.
[40] C. Kunusch, P. Puleston, M. Mayosky, and J. Riera, "Sliding mode strategy for PEM fuel cells stacks breathing control using a super–twisting algorithm," *IEEE Trans. Control Syst. Technol.*, vol. 17, no. 1, pp. 167–174, Jan. 2009.
[41] H. K. Khalil, *Nonlinear Systems*. Upper Saddle River, NJ, USA: Prentice-Hall, 1996.
[42] P. A. Ioannou and P. V. Kokotovic, *Adaptive Systems With Reduced Models*. New York, NY, USA: Springer-Verlag, 1983.

BYUNG MO KIM received the B.S. degree from the School of Electrical and Electronics Engineering, Chung-Ang University, Seoul, South Korea, in 2019, where he is currently pursuing the master's degree with the Department of Electrical and Electronic Engineering. His current research interests include nonlinear adaptive control and intelligent control using neural networks.

YUN HO CHOI received the B.S. degree in mechanical engineering and the Ph.D. degree in electrical and electronic engineering from Chung-Ang University, in 2013 and 2019, respectively. He is currently a Postdoctoral Researcher with the Department of Electrical and Electronic Engineering, Chung-Ang University. His research interests include nonlinear control systems and intelligent control systems using fuzzy logic systems and neural networks.

SUNG JIN YOO received the B.S., M.S., and Ph.D. degrees in electrical and electronic engineering from Yonsei University, Seoul, South Korea, in 2003, 2005, and 2009, respectively. He was a Postdoctoral Researcher with the Department of Mechanical Science and Engineering, University of Illinois at Urbana–Champaign, Illinois, from 2009 to 2010. Since 2011, he has been with the School of Electrical and Electronics Engineering, Chung-Ang University, Seoul, South Korea, where he is currently a Professor. His research interests include nonlinear adaptive control, decentralized control, distributed control, fault-tolerant control, neural networks theories, and their applications to robotics, flight, nonlinear time-delay systems, large-scale systems, and multiagent systems.